We are IntechOpen, the world's leading publisher of Open Access books Built by scientists, for scientists

4,800
Open access books available

122,000
International authors and editors

135M
Downloads

Our authors are among the

154
Countries delivered to

TOP 1%
most cited scientists

12.2%
Contributors from top 500 universities

BOOK CITATION INDEX
CLARIVATE ANALYTICS
INDEXED

WEB OF SCIENCE™

Selection of our books indexed in the Book Citation Index
in Web of Science™ Core Collection (BKCI)

Interested in publishing with us?
Contact book.department@intechopen.com

Numbers displayed above are based on latest data collected.
For more information visit www.intechopen.com

Structural Diversity Problems and the Solving Method for Antibody Light Chains

Emi Hifumi, Hiroaki Taguchi, Ryuichi Kato,
Mitsue Arakawa, Yoshiki Katayama and Taizo Uda

Additional information is available at the end of the chapter

Abstract

The structural diversity (heterogeneity) problem of antibodies has become a big subject along with the development of antibody drugs and catalytic antibodies. The detailed studies on the subject have not been conducted because many difficult and complex problems are existed in the phenomena. The heterogeneity problem is observed in a whole antibody as well as a catalytic antibody. The difficulty and complexity of the heterogeneity are in the generation of many isoforms caused by different charges, different molecular sizes, and/or modifications of amino acid residues. We found that the constant region domain of the antibody light chain also plays an important role in the heterogeneity. It is desirable that the antibody and/or the subunits must have a defined structure for practical use. We found interesting phenomena that copper ion can convert the multi-molecular forms of antibodies to mono-molecular forms. The ion contributed greatly to the enrichment of the dimer-form and the homogenation of the differently charged full-length and constant region domain of the light chain. The role of copper ion must be significant for preparing a single, defined, not multiple, isoform structure. Note that the big problem could be solved by using copper ion during the purification process.

Keywords: charge heterogeneity, 2D electrophoresis, antibody light chain, pI, copper ion

1. Introduction

In recent year, many monoclonal antibody drugs have been developed, and some of them are practically used in therapy [1–3]. With respect to catalytic antibodies, they have extensively been

developed [4–14] for the last two decades from the viewpoint of both basic research and the application, where it has been proved that there are many catalytic antibodies being effective against anti-rabies virus [15], anti-influenza virus [16], anti-*Helicobacter pylori* [17], anti-HIV [7, 8, 10], anti-Alzheimer's disease [14, 18], etc. Interestingly, some of them have been advanced to the stage tested *in vivo* in this decade [15–19]. In the case of catalytic antibodies, some of them play the role as a whole structure of IgG [5, 9, 11, 13], IgA [20], or IgM [21–23]. On the other hand, in some cases, their subunits (light chain or heavy chain) exhibit unique functions [1–4, 6–8, 12]. Once the antibody subunits are separated, the structure of the light or heavy chain becomes flexible and has a tendency to possess structural diversity (or molecular heterogeneity). Regarding structural heterogeneity, it was found about 20 years ago that a whole antibody possesses the structural heterogeneity. These studies were extensively studied by Harris et al. [24] and Nebija et al. [25] using the capillary isoelectric focusing and the 2D-gel electrophoresis [26, 27].

We have also reported about the molecular heterogeneity caused by different electrical charges and different molecular size in mouse monoclonal antibody [28]. This phenomenon is not good for the preparation efficacy, high reproducibility, and practical application. In addition, the structural diversity leads us to ask what structure plays the most important role in exhibiting the catalytic antibody functions. It also provides us with another subject of how we can best make a significant structure with high reproducibility and productivity.

We have recently found a crucial method to solve the heterogeneity problem by using copper ion, which can convert the multi-molecular forms into mono-molecular forms for many recombinant human antibody light chains. In addition, the constant region domain of the light chain (CL) plays an important role in generating a mono-molecular form.

In this review, we will describe a novel method for preparing a single and defined mono-form structure in detail.
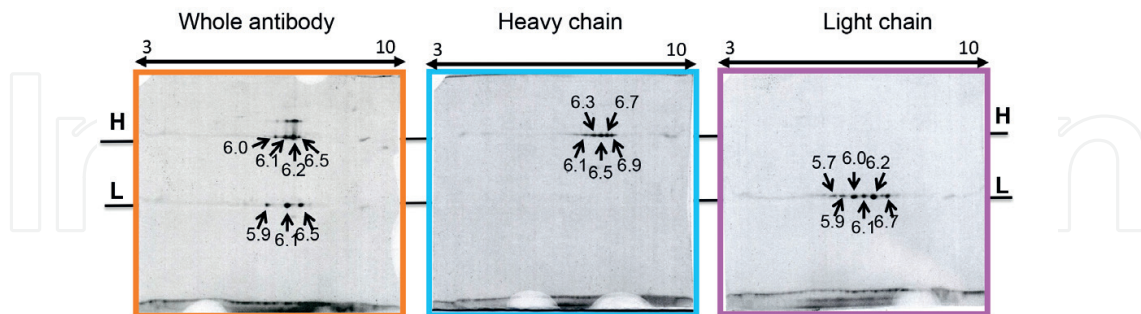
2. Structural heterogeneity of monoclonal antibodies

2.1. Examples found in natural monoclonal antibodies

We have found an interesting phenomenon in 2D-gel electrophoresis for mouse type monoclonal antibodies (mAbs), which were prepared against the hemagglutinin molecule of influenza virus [29]. In the experiment, these monoclonal antibodies showed many different spots at the same molecular size [28]. **Figure 1a** shows the results using InfA-9 mAb. In the case, the whole antibody and the subunits, heavy and light chains separated and purified from the parent whole antibody, were analyzed by 2D-gel electrophoresis. In **Figure 1a**, many spots in the whole antibody of InfA-9 are shown. The clear four spots (pI = 6.0, 6.1, 6.2 and 6.5) in the heavy chain and three spots (pI = 5.9, 6.1 and 6.5) in the light chain were detected. Except these spots, many faint spots were observed in the same molecular size (the spots observed over the heavy chain were unknown). Then, the heavy and light chains were separated from the whole antibody of InfA-9, highly purified, and submitted to 2D-gel electrophoresis. The results exhibited the similar phenomena. In the heavy chain, similar spots are seen, and clear five spots (pI = 6.1, 6.3, 6.5, 6.7 and 6.9) were detected in this case. The pI positions of the spots
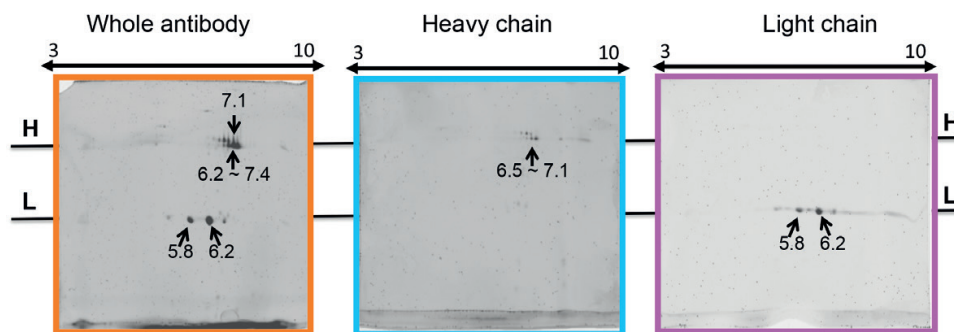
a)

b)

Figure 1. 2D electrophoresis for mouse type monoclonal antibodies against hemagglutinin molecule of influenza virus. SDS-PAGE; Running gel 12.5%. Strip; pH 3–10 nonlinear 7 cm. Sample; whole antibody 3.2 μg, heavy and light chain: 1.6 μg. Staining; deep purple (GE Healthcare). (a) InfA-9 monoclonal antibody. Whole antibody: many spots are seen in the whole antibody of InfA-9. The clear four spots (pI = 6.0, 6.1, 6.2 and 6.5) in the heavy chain and three spots (pI = 5.9, 6.1 and 6.5) in the light chain were detected. Heavy chain (H): clear five spots (pI = 6.1, 6.3, 6.5, 6.7 and 6.9) were detected. The pI positions of the spots were a little bit different compared to the whole antibody. Light chain (L): clear six spots (pI = 5.7, 5.9, 6.0, 6.1, 6.2 and 6.7) were detected. The number of spots increased compared with those of the whole antibody. (b) InfA-15 monoclonal antibody. For the whole antibody and the heavy and light chain, similar results showing many spots at different pI for the same molecular sizes were observed, suggesting that the molecular heterogeneity of antibodies are generally occurring events.

were a little bit different compared to the whole antibody. For the case of the light chain, clear six spots (pI = 5.7, 5.9, 6.0, 6.1, 6.2 and 6.7) were detected. The number of spots increased compared with those of the whole antibody. These phenomena are not exceptional, but general. The mAb, InfA-15, exhibited similar results. **Figure 1b** shows 2D-gel electrophoresis using InfA-15 mAb. In the results of the whole antibody and the heavy chain and the light chain, the pattern of spots were a little different from those of InfA-9 mAb, but several different pI spots were observed in all cases. Namely, different pI spots are present at the same molecular size in any mAb. Note that structural diversity (molecular heterogeneity) should be existing even in the monoclonal antibody and the subunits, while they are a single protein. In our case, it is considered that the various electrical charges of the molecule may be one of the causes.

2.2. Recombinant monoclonal antibody Herceptin

The structural diversity of antibodies has been found about 20 years ago [26, 27], suggesting that an antibody has some different structures (not a mono-form structure) caused by the various electrical charges. Regarding the charge heterogeneity, Harris et al. [24] and Nebija et al. [25, 30] have extensively studied this phenomenon with recombinant antibodies using capillary isoelectric focusing and 2D-gel electrophoresis.

The former paper [24] pointed out a deamidation of Asn residues in the protein.

The latter papers showed multiple spots of pI spreading at heavy and light chains, caused by generation of charge-related isoforms. The pI spreading pattern in 2D-gel electrophoresis [30] is similar to our cases. The effects of sugar chains are also taken into account for molecular heterogeneity.

As it is well known that an antibody light chain has no sugar chain, this can be excluded for this subunit. Thus, in our case, it is thought that the structural diversity is mostly due to the heterogeneity of the different electrical charges. In addition, the possibility of deamidation is excluded because it is hardly considered that the addition of a copper ion causes a reverse reaction of the deamidation and the heterogeneity is lost.

3. Structural heterogeneity of recombinant human antibody light chains (including catalytic light chains)

3.1. Phenomena observed in several human antibody light chains

3.1.1. Chromatograms of antibody light chain C51

In this section, we will describe the phenomena of structural diversity using full-length light chains of human antibodies. **Figure 2a** shows the amino acid sequences of human antibody kappa light chains of C51, #4 and #7. The proteins were expressed in *Escherichia coli* in accordance with the protocol described in the section of Materials and Methods in Refs. [19, 31, 32]. Methionine was adducted at the N-terminus and confirmed by amino acid sequence analysis after cloning the cDNA of the light chain into the *Nco I* site of the pET-20b vector. Leu and Glu residues were inserted by employing the *Xho I* site before a histidine–tag (His × 6) included in the vector for purification.

After the transformed *E. coli* cells were recovered by centrifugation, they were sonicated. Then, the soluble fraction was subjected to purification using Ni-NTA affinity chromatography. The result of a Ni-NTA affinity chromatography for the C51 light chain is shown in **Figure 2b**. The C51 light chain was eluted from fraction 28 (Fr.28) to Fr.44. Fr.35 showed the maximum absorbance. Fr.35 was collected and analyzed by SDS-PAGE with CBB staining, where the C51 light chain was mainly the monomer form with a slight contamination of dimer forms.

The eluted fractions from Fr.30 to Fr.40 were collected and subjected to a cation exchange chromatography. **Figure 2c** shows the chromatogram, where several peaks were observed. The SDS-PAGEs of the peaks were shown in the figure on the right side. The peaks 1, 2, and 3 were the monomer, the mixture of monomer and dimer, and the dimer, respectively.
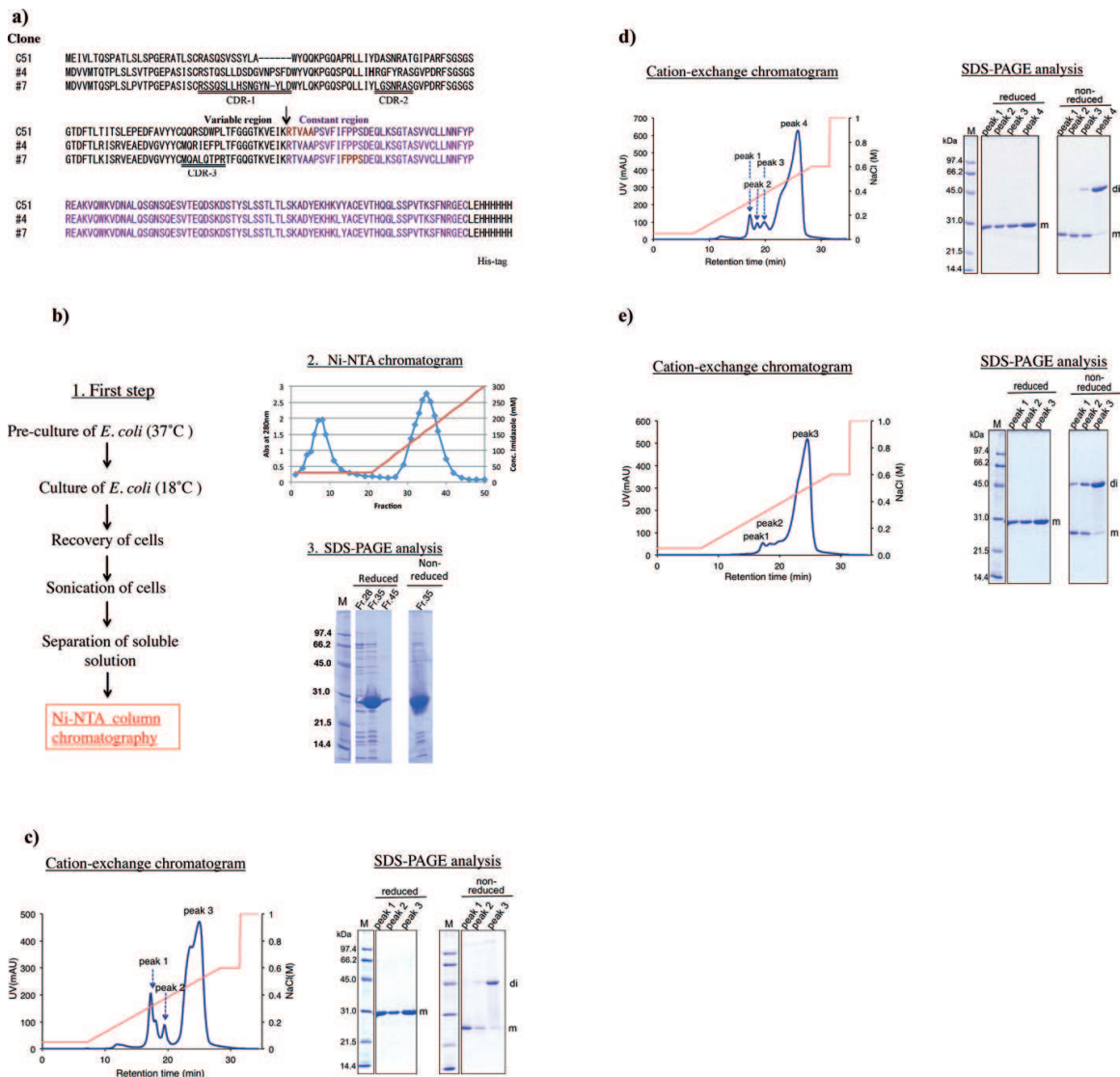
Figure 2. C51 light chain. (a) Amino acid sequences of human light chains (kappa type). (b) First-step purification of C51 light chain. (b-1) Steps from *E. coli* culture to Ni-NTA column chromatography. (b-2) Ni-NTA column chromatogram for C51 light chain. (b-3) Results of SDS-PAGE of fraction 28–45. C51 light chain was mainly the monomer form with a slight contamination of dimer forms at approximately 45 kDa. (c) Cation exchange chromatography as the second-step purification without copper ion. Several peaks were observed from 15 to 27 min. The peaks 1, 2, and 3 were the monomer, the mixture of monomer and dimer, and the dimer, respectively. (d) Cation exchange chromatography as the second-step purification with addition of 0.5 eq. copper ion in cell suspension. A main peak (peak 4) was observed at the retention time of 26 min but other peaks (1–3) were small. The SDS-PAGE gave a dimer for peak 4. (e) Cation exchange chromatography as the second-step purification with addition of 0.5 eq. copper ion in the Ni-NTA eluent. Only a main peak (peak 3) was observed at the retention time of 26 min but other peaks (1 and 2) were scarcely detected. The SDS-PAGE gave a dimer for peak 3. The addition of Cu^{2+} led to formation of dimers.

3.1.2. Effect of copper ions

Twenty μM of $CuCl_2$ (Cu^{2+}) was added to either the cell suspension after recovery of the cells (cell-suspension) or the eluent of Ni-NTA chromatography (Ni-NTA eluent). By the addition of Cu^{2+} to the cell suspension, the chromatogram changed to that shown in **Figure 2d**, where a main peak (peak 4) was observed at the retention time of 26 min but other peaks (1, 2 and 3) were small. The SDS-PAGE gave a dimer for peak 4. In **Figure 2e**, 20 μM of Cu^{2+} (0.5 equivalent to the light chain)

was added to the Ni-NTA eluent. In this case, only a main peak (peak 3) was observed at the retention time of 26 min but other peaks (1 and 2) were scarcely detected. The SDS-PAGE gave a dimer for peak 3. The addition of Cu^{2+} led to dimer formation.

Mass spectroscopic (MS) analysis was performed for the main peaks observed above (data not shown). Briefly, a monomeric light chain was detected at 25,000 m/z and a dimer at 49,000 m/z. A small trimer and tetramer were also detected at 74,000 and 98,000 m/z, respectively. By the addition of Cu^{2+} to the cell suspension or the Ni-NTA eluent, the signal for the monomer was substantially reduced. Conclusively, the addition of Cu^{2+} was effective for the formation of the dimer.

In order to examine the pI of the light chain, 2D-gel electrophoresis was performed with and without the addition of Cu^{2+}. The results are shown in **Figure 3a** and **b**. In the case without Cu^{2+}, many spots at different pIs were observed with the same molecular size of 31 kDa (**Figure 3a**). The pI spots were widely located from 6.12 to 10.0. The strong spot was observed at pI = 6.45–6.73. In contrast, in the case with the addition of Cu^{2+}, the spots were gathered on the strongest spot at pI = 6.57, while two faint spots were detected at around pI = 6.32 and 6.90 (**Figure 3b**). It is evident that the electrical charges of the molecule became mono-form by the effect of Cu^{2+}.

3.2. #4 and #7 light chains

It must be invested whether or not the changes from multi-molecular forms to mono-molecular forms by the addition of copper ions is a general phenomenon. The following experiments were carried out.

3.2.1. Chromatograms

For the purpose of confirmation of the observed phenomena on the structural diversity, other antibody light chains such as #4 and #7 were examined. As stated above, the chromatogram in Ni-NTA purification is similar for many light chains. Thus, the following is focused on the results of cation exchange chromatography, which were very different in each light chain used. The effect of copper ions on the diversity issue will be discussed.

The cation chromatograms for #4 light chain are shown in the cases without and with Cu^{2+} as presented in **Figure 4a** and **b**, respectively. In the case without Cu^{2+}, there were several peaks. The results of SDS-PAGE (non-reduced condition) corresponding to three peaks are also shown. The observed peaks were a mixture of monomers and dimers. Namely, several structurally different light chains caused by different electrical charges are coexisting in the solution. However, when 20 μM of Cu^{2+} (0.5 equivalent to the light chain) was added to the Ni-NTA eluent, the several peaks in **Figure 4a** surprisingly became a single peak (**Figure 4b**), which was mainly the dimer.

In the case of the chromatography for #7 light chain, huge three peaks were observed in the case without Cu^{2+} as shown in **Figure 5a**. The peak of the retention time at 9 min was the monomer. The peak at 13 min was a mixture of monomer and dimer. The peak at 22 min was also a mixture. Note that light chains possess different molecular sizes and electrical charges in solution.
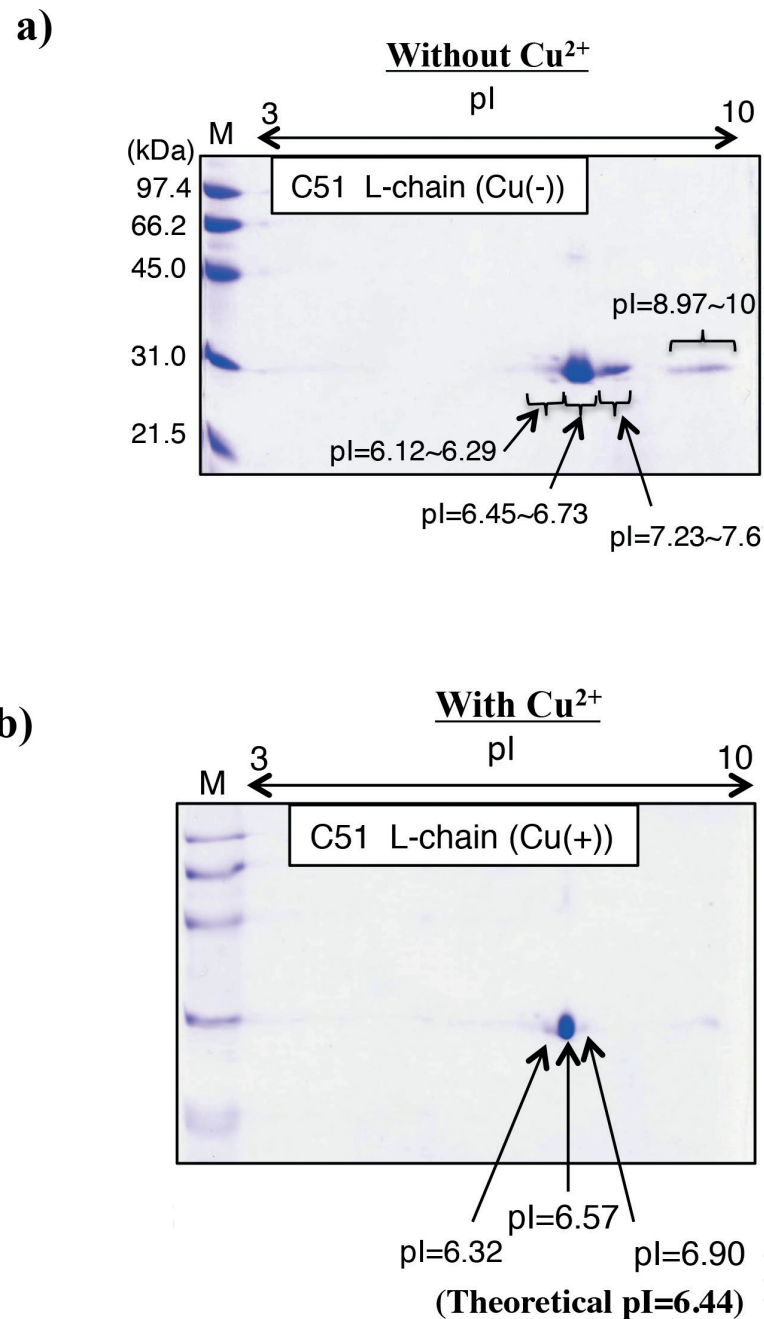
Figure 3. 2D-gel electrophoresis for C51 light chain. (a) Without copper ion. The pI spots were widely located from 6.12 to 10.0. (b) With copper ion. The spots were gathered on the strongest spot at pI = 6.57, although two faint spots were detected at around pI = 6.32 and 6.90.

When 15 μM of Cu^{2+} (0.38 eq.) was added to the Ni-NTA eluent, two peaks at 12 min and 23 min of retention time were observed in the chromatography. The results of SDS-PAGE analysis (**Figure 5b**) indicated that both peak A and peak B were dimers. It is interesting that two kinds of dimers with different electrical charges were coexisting. When 40 μM of Cu^{2+} (1.0 eq.) was added to the same eluent, only peak C, which corresponds to peak A in **Figure 5b**, was observed at 12 min and peak B was not detected (**Figure 5c**). It is thought that peak B moved to peak A in **Figure 5b**. Conclusively, the dimeric light chains possessing two kinds of electrical charges became one kind of state possessing a unique electrical charge by the addition of 40 μM of Cu^{2+}.
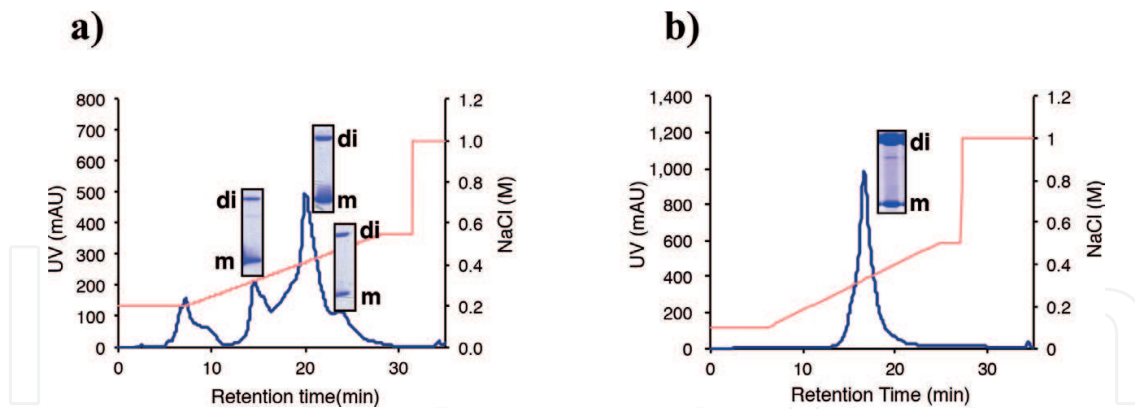
Figure 4. Cation exchange chromatography for #4 light chain. (a) Without copper ion. There were mainly three peaks, which were a mixture of monomers and dimers. Namely, several structurally different light chains caused by different electrical charges are coexisting in the solution. (b) With copper ion of 0.5 eq. When 0.5 equivalent to the light chain was added to the Ni-NTA eluent, the several peaks became a single peak of mainly the dimer.
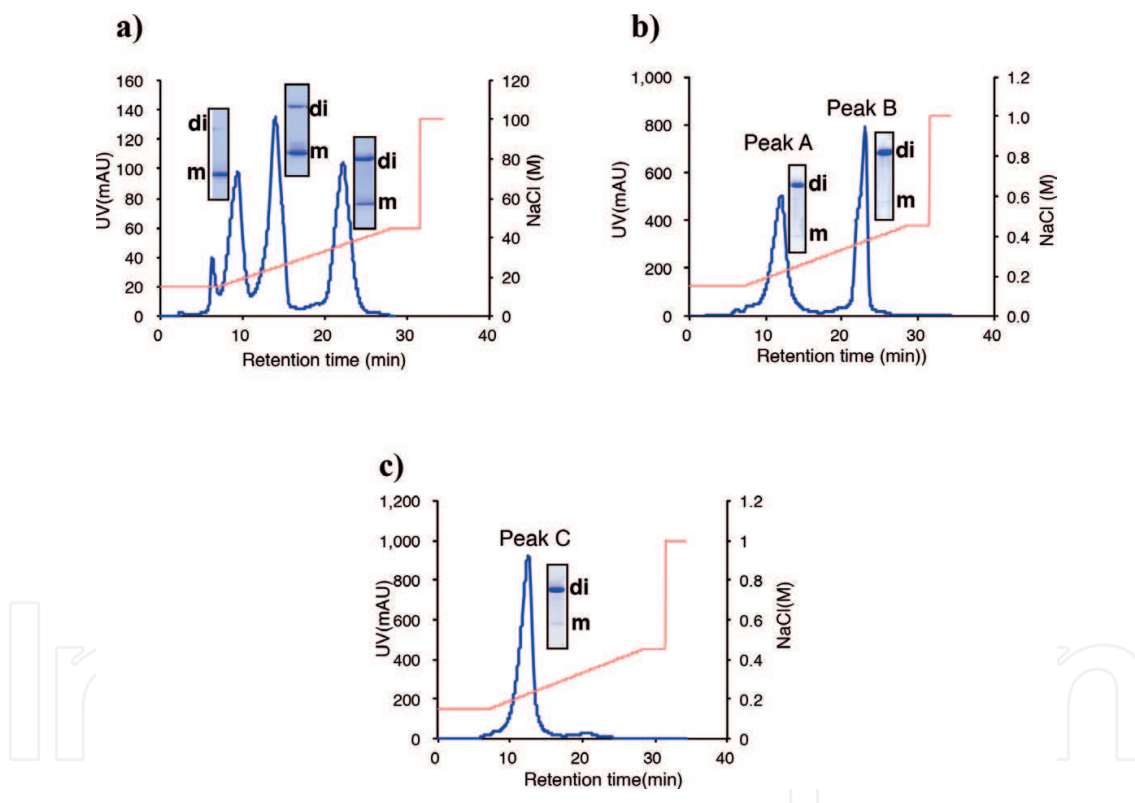

Figure 5. Cation exchange chromatography for #7 light chain. (a) Without copper ion. Huge three peaks were observed. The peak of the retention time at 9 min was the monomer, peak at 13 min was the mixture of monomers and dimers, and peak at 22 min was a mixture. In this case, the light chains possess different molecular sizes and electrical charges in solution. (b) With copper ion of 0.38 eq. Two peaks at 12 min and 23 min retention time were observed and both peak A and peak B were dimers. (c) With copper ion of 1.0 eq. Only peak C, which corresponds to peak A in (b), was observed at 12 min as the dimer form.

A chemical analysis of Cu^{2+} gave interesting results. The ratio of Cu to light chain (Cu/light chain) is 0.48, 0.03, and 0.64 for peaks A, B and C, respectively. When the ratio of Cu/light chain was 0.48 in **Figure 5b** and 0.64 in **Figure 5c**, the dimer was eluted at 12 min. In contrast, at a ratio of 0.03, the retention time was 23 min. These results suggest that whenever enough Cu^{2+} is present in the solution, an electrically homogeneous light chain could be observed at a retention time of 12 min.

UV/VIS spectroscopy for these peaks was also conducted. The results are shown in **Figure 6**. We could see the absorbance around 560 nm, which is assigned to the absorbance of the interaction of cupper with the amino acids for peak A and peak C, but not for peak B, whose spectrum was very similar without copper ion.

3.2.2. AFM analysis

In order to investigate the morphology of antibody light chains, we conducted atomic force microscopy (AFM) analysis. The peaks of A, B, and C were collected and subjected to AFM analysis as shown in **Figure 7a–c**. **Figure 7a** shows the AFM image for peak A. The images for peak B and C are shown in **Figure 7b** and **c**, respectively. The red circle represents the clear image of the dimeric light chain. The size of the dimer was roughly estimated at an
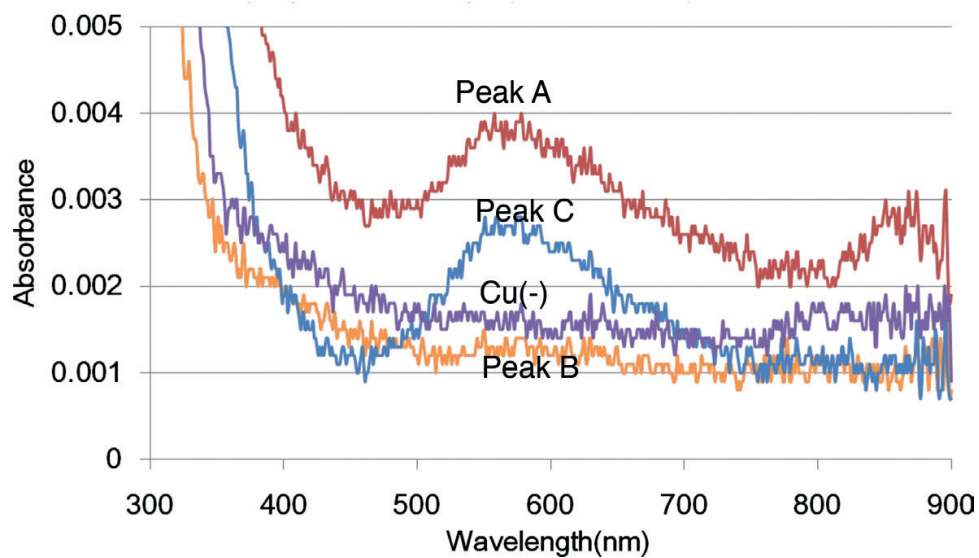

Figure 6. UV/VIS spectroscopy. The absorbance around 560 nm, which is assigned to the absorbance of the interaction of a copper ion with the amino acids, was observed for peak A and peak B, but not for peak B. It is obvious that peak B has no copper ion.
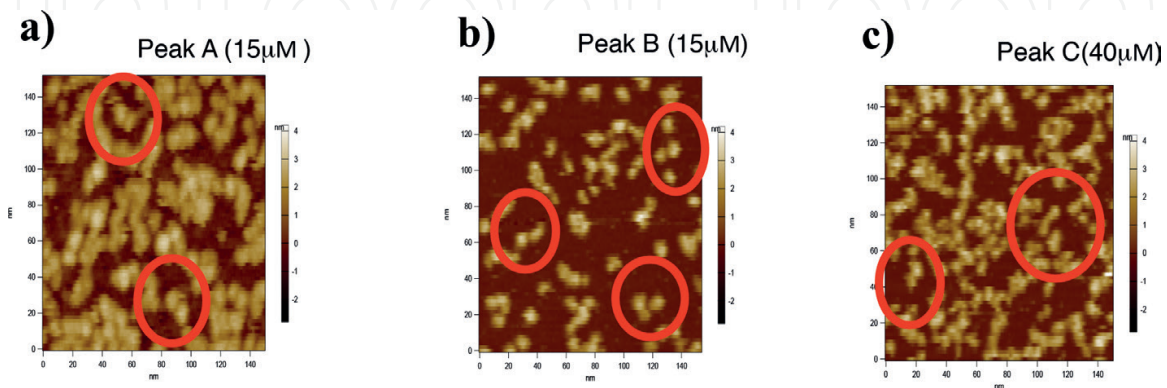

Figure 7. AFM analysis. The peaks of A, B, and C were collected and subjected to AFM analysis. The red circle represents the clear image of the dimeric light chain. (a) Peak A included Cu^{2+} with the ratio of Cu/#7 light chain = 0.48. (b) Peak B did not include Cu^{2+} (Cu/#7 light chain = 0.03). (c) Peak C included Cu^{2+} with the ratio of Cu/#7 light chain = 0.64. The size of the dimer was roughly estimated at an approximate length of 20 nm, the width of 10 nm, and the height of 4 nm.

approximate length of 20 nm, the width of 10 nm, and the height of 4 nm. The lateral and height length are comparable with the AFM image of IgG by Querghi et al. [33]. We could not identify the position of the copper ion residing in the light chain from this AFM analysis.

4. Structural heterogeneity of the constant region domains of light chains (CLs)

In the previous section, we focused on a full-length light chain, which is consisted of the variable and the constant domain. It is noteworthy to study which domain, the former or latter, causes the structural diversity problem. Although there are many studies on the role of the constant domains (especially for a Fc region) of the heavy chain of the antibody, the reports on the role of the constant region domain of the light chain are scarcely seen. From this point of view, we investigated the role of the constant domain as described in the following.

4.1. Sequence of the constant region domain of a human antibody light chain

Figure 8 shows the amino acid sequence of the recombinant constant region domain (kappa type) of a human antibody light chain employed in this study. Methionine (M) and alanine (A) at position nos. 1 and 2 of the aa sequence have been inserted by cloning using the restriction enzyme *Nco I*. Underlined is the sequence of the constant region domain. Arginine (R) at position no. 3 is the first amino acid residue of the constant region. Leucine (L) and glutamic acid (E) before His × 6 were also inserted by using the restriction enzyme (*Xho I*).

4.1.1. Chromatography and SDS-PAGE analysis

The expression and purification of the kappa type constant domain were similarly conducted as made in the full-length light chain. Ni-NTA chromatography was also performed to purify the recovered constant region domain. The result was also similar with that obtained in the case of full-length light chain except for the molecular size. The SDS-PAGE analysis for the collected fraction in the Ni-NTA chromatography is shown in **Figure 9**. Under non-reduced condition, a strong band was detected in the monomeric form at 15 kDa as well as a weak band in the dimeric form at 30 kDa. Under reduced condition, only the monomeric form was observed and the purity was over 95%. This sample was applied to cation exchange chromatography.

MARTVAAPSVFIFPPSDEQLKSGTASVVCLLNNFYPREAK
VQWKVDNALQSGNSQESVTEQDSKDSTYSLSSTLTLSKAD
YEKHKVYACEVTHQGLSSPVTKSFNRGECLEHHHHHH

Figure 8. Amino acid sequence of the constant region domain of a human antibody light chain (kappa type). Underlined is the aa sequence of the constant region domain of the kappa light chain. Methionine (M) and alanine (A) of the aa sequence at the first and second position were inserted by cloning using the restriction enzyme *Nco I*. Arginine (R) at the third position is the first amino acid residue of the constant region. Leucine (L) and glutamic acid (E) before His × 6 were also inserted by cloning using the restriction enzyme *Xho I*.
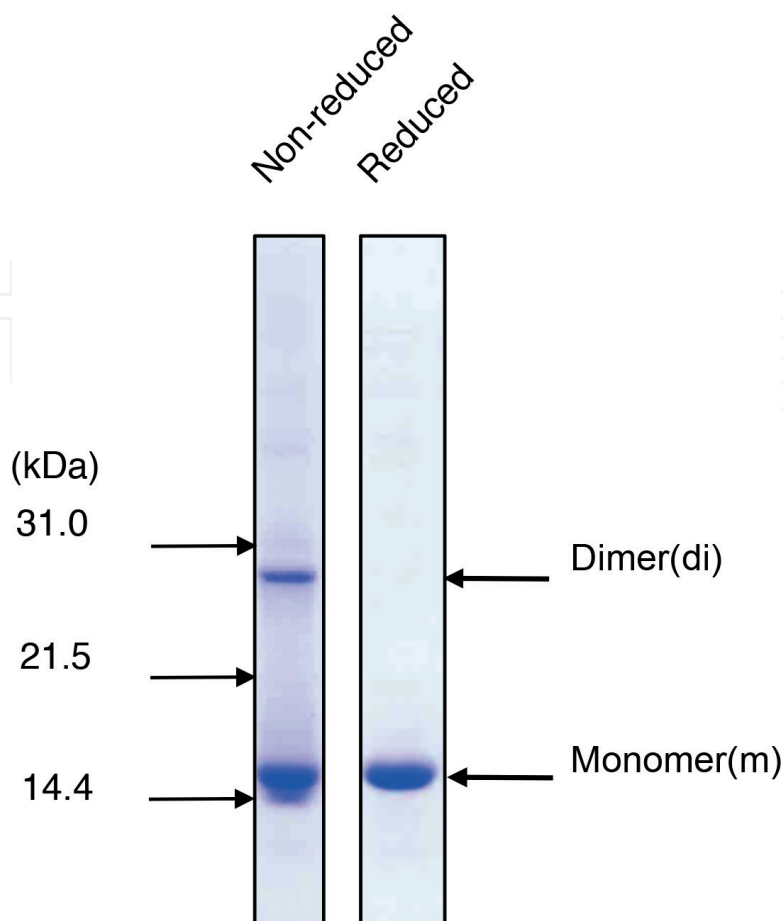
Figure 9. SDS-PAGE of the constant region domain after Ni-NTA chromatography. Under non-reduced condition, a strong band was detected in the monomeric form at 15 kDa as well as a weak band in the dimeric form at 30 kDa. Under reduced condition, only the monomeric form was observed and the purity was over 95%.

The results are shown in **Figure 10** along with the SDS-PAGE analysis under non-reduced condition. Several peaks were observed at retention times from 5 to 25 min while it was a single material of the constant domain. In **Figure 10**, peak 1 appearing at the retention time of 7.5 min is a monomer, and peaks 2, 3, and 4 appearing at 14–17 min contain mainly monomers. The dimers or/and trimer were detected for peaks 2 and 4. Peaks 5 and 6 appearing at 21–23 min are the dimer. These results mean that differently charged molecules of the constant region domain as well as differently sized molecules coexisted in solution at the same time. It is obvious that a constant region molecule shows molecular heterogeneity (structural diversity) from the viewpoint of both electrical charge and molecular size, which are very similar with those observed in the full-length light chain.

4.2. Effect of copper ions

As stated previously, copper ion (Cu^{2+}) hugely influenced the structural diversity of the full-length light chain. The same experiment was performed with the constant region domain molecule. The results are summarized in **Figure 11a–f**. In the case of 0.1 eq. addition of Cu^{2+} for the constant region domain molecule, we observed a small peak 7 and one main peak
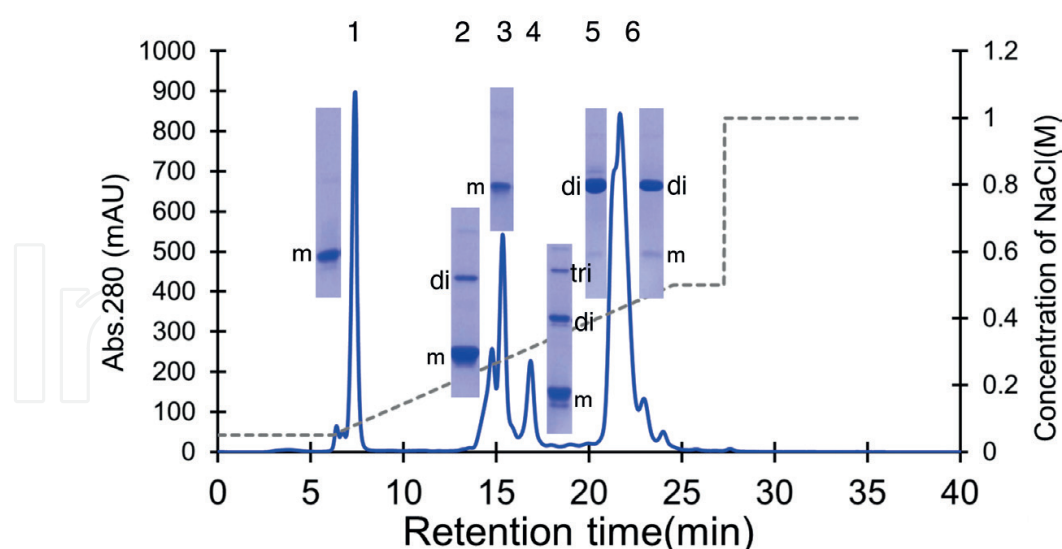
Figure 10. Cation exchange chromatography for the constant region domain molecule of the light chain (CL). Peak 1 appearing at the retention time of 7.5 min is a monomer and peaks 2, 3, and 4 appeared at 14–17 min contain mainly monomers. The dimers or/and trimer were detected for peaks 2 and 4. Peaks 5 and 6 appearing at 21–23 min are the dimer. These results mean that differently charged molecules of the constant region domain as well as differently sized molecules coexisted in solution at the same time. This result was very similar with that observed with the full-length light chain.

8, which were eluted at the retention time around 16 and 22 min, respectively (**Figure 11a**). Peak 8 was the dimer by the SDS-PAGE analysis under non-reduced condition (peak 7 was not analyzed because of the small peak). In the case of 0.2 eq. addition of copper, mainly two peaks (9 and 10) were obtained (**Figure 11b**). The elution times of peaks 9 and 10 were identical with those of peaks 7 and 8, respectively. Peak 9 included mainly the dimer with a very slight amount of the monomer. Peak 10 was the dimer. For these two peaks, UV/VIS spectroscopy was performed. The results are presented in **Figure 12**. Peak 9 showed an absorbance of around 580 nm, which was based on the interaction of Cu^{2+} and amino acids of the constant region domain molecule. On the other hand, no absorbance was detected for peak 10. Namely, protein of peak 9 bound to Cu^{2+} but peak 10 did not. Though the peaks are dimeric forms of the constant region domain, they were separated by the cation exchange column chromatography whether or not the peak contains Cu^{2+}. For the case of 0.3 eq. addition, the main peak was peak 11 observed at the retention time of 16 min, which included the dimer along with a slight monomer and trimer forms (**Figure 11c**). In the case of 0.4 eq. addition, a clear single peak of the dimer form was detected at the retention time of 16 min (**Figure 11d**). In **Figure 11e** and **f**, peaks 13 and 14 were observed as single peak at the retention time of 16 min. And they were the dimer. It seems that enough content of added copper ion was 0.4 eq. to induce mono-form formation from the multi-forms of the constant region domain molecule.

The amount of Cu^{2+} bound to the constant region domain molecule was also quantified using a commercially available copper detection kit (Copper, Low Concentration, Assay Kit, AKJ, CU21M, Metallogenics Co., Ltd., Chiba, Japan). For the peak appearing at the retention time of 16 min and containing Cu^{2+}, the ratio of Cu^{2+}: constant region domain was around 0.55. This result agreed with those of the UV/VIS spectroscopy, suggesting that two constant region domain molecules bind one copper ion.
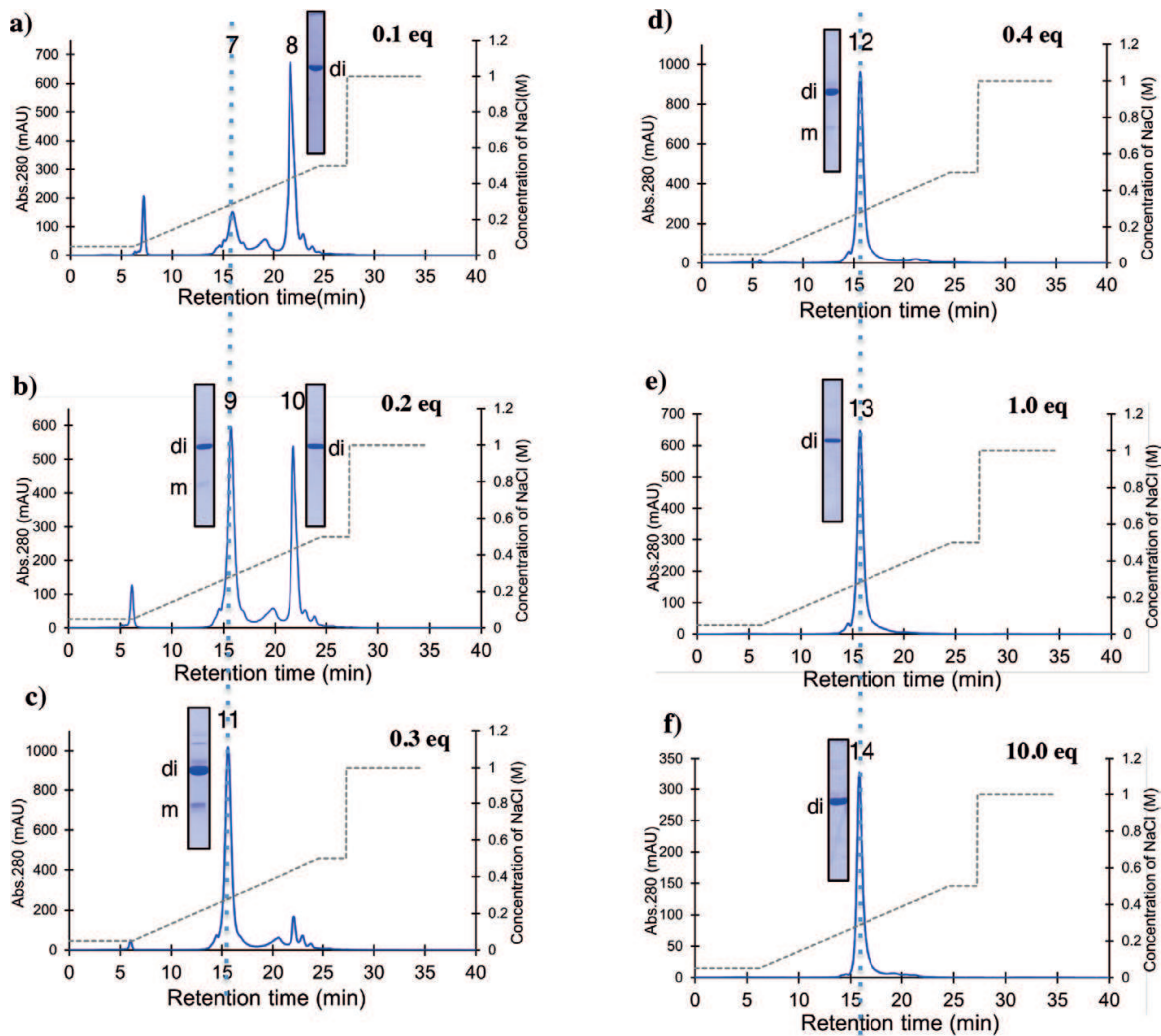
Figure 11. Effect of copper ions. (a) 0.1 eq. addition of Cu^{2+}: a small peak 7 and one main peak 8 were observed at the retention time around 16 and 22 min, respectively. Peak 8 was the dimer. (b) 0.2 eq. addition of Cu^{2+}: the eluted times of peaks 9 and 10 were identical with those of peaks 7 and 8, respectively. Peak 9 included mainly the dimer with a very slight contamination of the monomer. Peak 10 was the dimer. (c) 0.3 eq. addition of Cu^{2+}: peak 11 was observed as the main peak at the retention time of 16 min. (d) 0.4 eq. addition of Cu^{2+}: A clear single peak of the dimer form was detected at the retention time of 16 min. (e) 1.0 eq. addition of Cu^{2+}: only peak 13 was observed at the retention time of 16 min. It was the dimer. (f) 10.0 eq. addition of Cu^{2+}: only peak 14 was observed at the retention time of 16 min. It was also the dimer. It seems that the amount of 0.4 eq. added copper ions is sufficient to induce the mono-molecular form from the multi-molecular forms of the constant region domain molecule.

4.3. Binding affinity of copper ions

The UV/VIS spectrum changed as different concentrations of Cu^{2+} was added to the Ni-NTA elution after the samples were dialyzed against PBS. The results are presented in **Figure 13**. The absorbance of 580 nm became larger along with an increase in the amount of added Cu^{2+}, as showing a slight red shift. In **Figure 14**, the values for the concentration of added Cu^{2+} were plotted vs. the maximum absorbance, which is the absorption isotherm curve for Cu^{2+} binding to constant region domain molecules. The Langmuir plot is shown in the inset of **Figure 14**, indicating a good linear relationship. The binding constant was estimated to be 48.0 μM^{-1}.
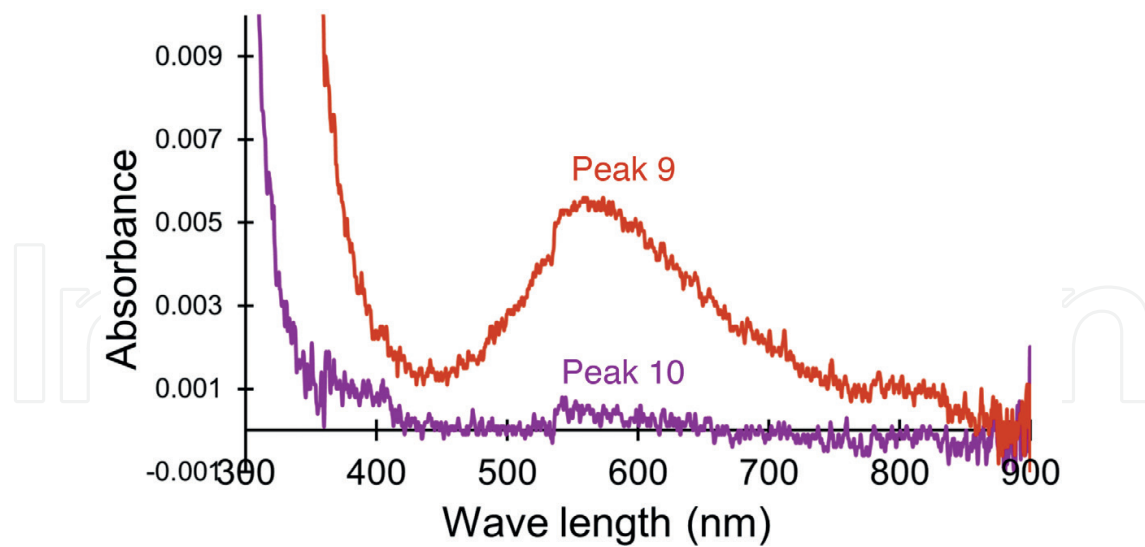
Figure 12. UV/VIS spectra. Peak 9 showed the absorbance of around 580 nm, which was based on the interaction of Cu^{2+} and amino acids of the constant region domain molecule. On the other hand, no absorbance was detected for peak 10.
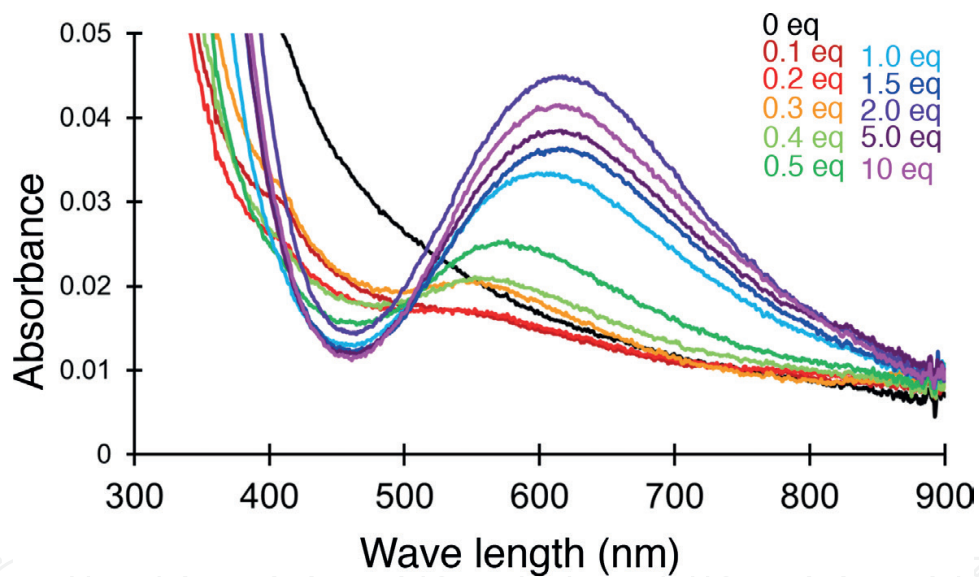

Figure 13. Spectrum changes with the concentration of added Cu^{2+}. Along with an increase of the concentration of added Cu^{2+}, the absorbance at around 580 nm became larger.

The binding affinity from several proteins incorporating divalent metal ions was investigated. The values (K) are presented in **Table 1**. Hemocyanin and metallothionein have very strong affinity to bind Cu^{2+}. Carbonic anhydrase-binding Zn^{2+} shows a strong affinity. Aminopeptidase III binding Co^{2+} possesses a weak affinity. In the case of CL, the value (48.0 μM^{-1}) seems to be intermediate among those metalloproteins.

In order to further investigate the molecular heterogeneity of the constant region domain molecule, two-dimensional (2D) electrophoresis was performed using samples with or without Cu^{2+}. **Figure 15a** and **b** shows the results for the cases without and with the addition of Cu^{2+}
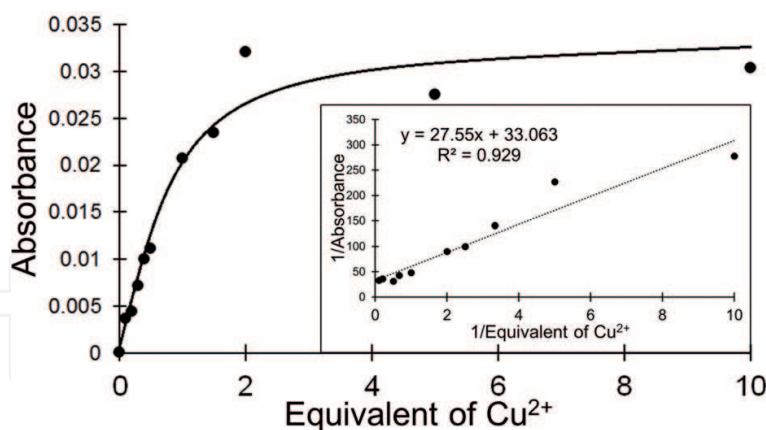
Figure 14. Kinetic analysis. The values for the concentration of added Cu^{2+} were plotted vs. the absorbance at 580 nm, which is the isothermal curve for copper binding to the CL protein. The Langmuir plot is presented in the inset of the graph, indicating a good linear relationship. The binding constant was estimated to be 48.0 μM^{-1}.

Proteins (metal ion)	K (M^{-1})	Affinity
Hemocyanin (Cu^{2+})	10^{17}–10^{19}	Very strong
Metallothionein (Cu^{2+})	10^{17}–10^{19}	Very strong
Carbonic anhydrase (Zn^{2+})	$\sim 10^{12}$	Strong
Aminopeptidase III (Co^{2+})	2×10^4	Weak
CL (Cu^{2+})	4.8×10^7	Medium

Table 1. Comparison of the binding affinities of some proteins with metal ions.

under non-reduced conditions, respectively. In the former case, many spots were observed: two spots at pI = 6.9 for the dimer and three spots at pI = 6.2, 6.5, and 6.9 for the monomer. In contrast, one strong spot was observed at pI = 6.9 for the dimer in the case with the addition of Cu^{2+}, while very faint spots were detected in the positions of the monomer. Note that Cu^{2+} can facilitate changes from the multimeric form to the monomeric form as well as from different electrical charges to a single electrical charge.

4.4. Other metal ions

About 1.0 eq. of a metal ion such as Ca^{2+}, Mg^{2+}, Ni^{2+}, and Zn^{2+} was added in each Ni-NTA elution and incubated overnight. **Figure 16** shows the results of the cation exchange chromatography and SDS-PAGE (non-reduced) for peaks P3 and P5. For the cases of Ca^{2+}, Mg^{2+}, and Ni^{2+} (**Figure 16a–c**, respectively), a large peak P3 was observed at 17 min along with a small peak P5 at 23 min. Interestingly, a large peak P3 was observed and peak P5 became very small in the case of Zn^{2+} (**Figure 16d**). The chromatogram resembled the case of Cu^{2+} (**Figure 16e**). From the results of the SDS-PAGE, the peak P3 was mostly in a monomeric form for all the cases of Ca^{2+}, Mg^{2+}, Ni^{2+}, and Zn^{2+}. On the other hand, P3 of Cu^{2+} was the dimer. The molecular form (size) of P3 in the case of Ca^{2+}, Mg^{2+}, Ni^{2+}, and Zn^{2+} was quite different from that of

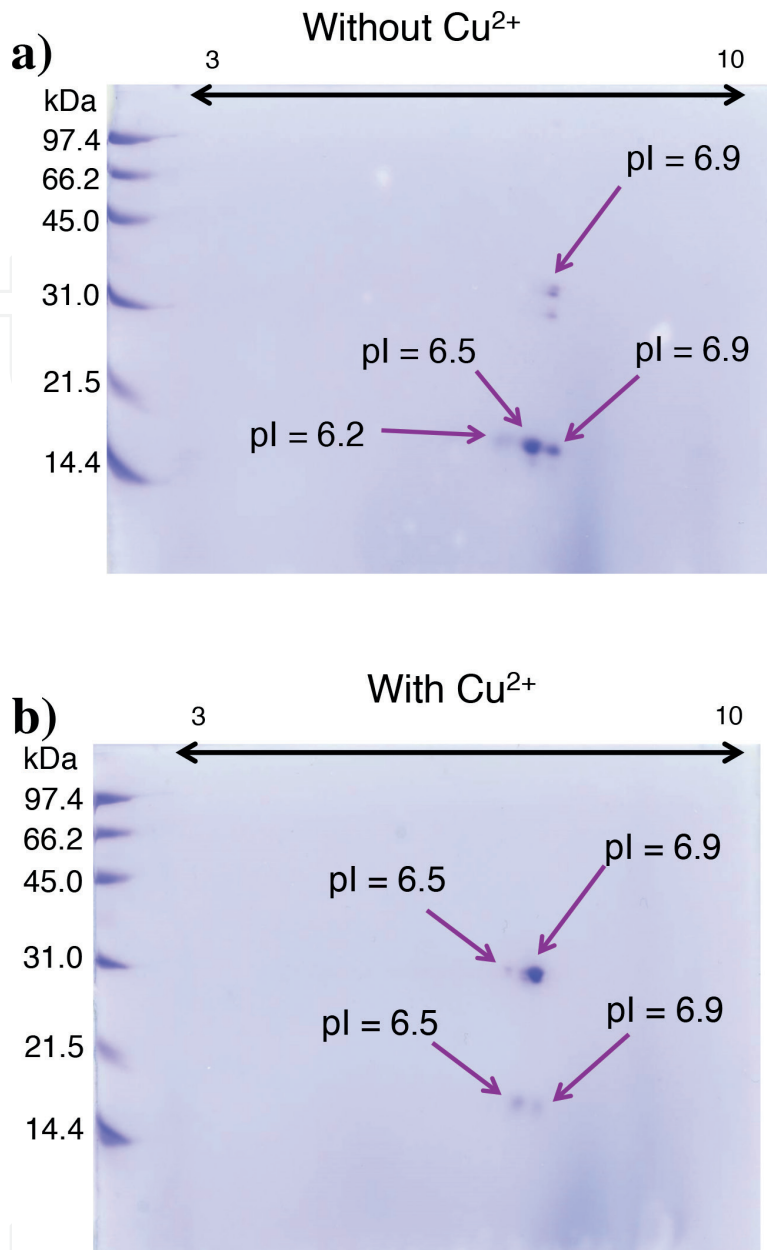**Figure 15.** 2D electrophoresis for the constant region domain (CL). (a) Without Cu^{2+}: two spots at pI = 6.9 for the dimer and three spots at pI = 6.2, 6.5, and 6.9 for the monomer were found. (b) With Cu^{2+}: one strong spot was observed at pI = 6.9 for the dimer. It is revealed that copper ion accelerates both dimerization and generation of a mono-molecular form of the light chain.

Cu^{2+}. It must be considered that the Zn^{2+} could not accelerate the dimerization of the constant region domain molecule, while the ion decreased the peak P5 and showed a large peak P3. Zn^{2+} could have some ability to unify the structural diversity, but the effect is different from that of copper.

Zn^{2+} did not accelerate the dimerization of the constant region domain molecule but has some functions that may contribute to solve the heterogeneity problem. Out of the several metals analyzed, Zn^{2+} exhibited an interesting behavior, which must be a characteristic feature
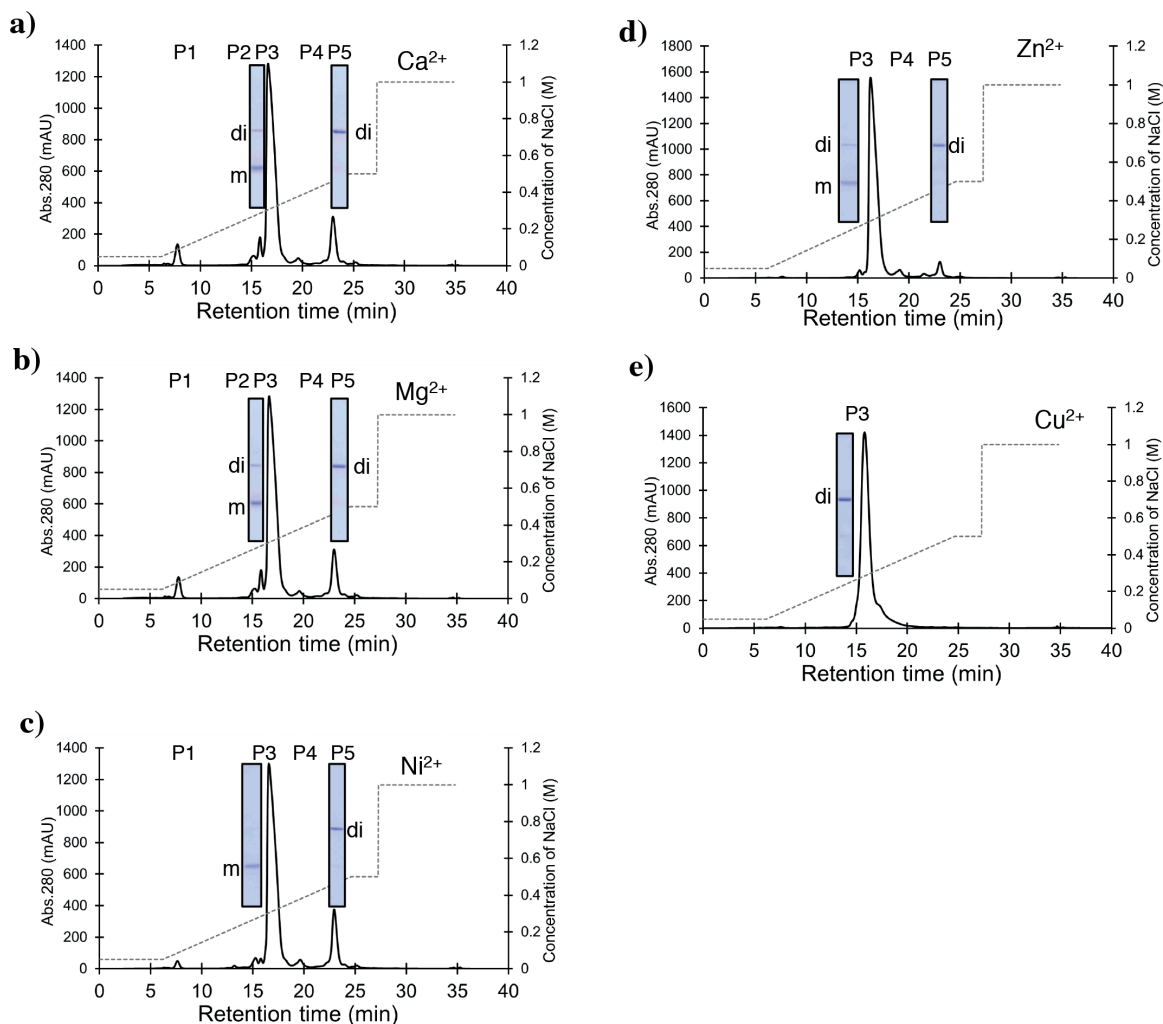
Figure 16. Other metal ions. In all cases, 1.0 eq. metal ion was added. Cation exchange chromatograms are presented with the results of SDS-PAGE (under non-reduced condition). m: monomer; di: dimer. (a) Addition of Ca^{2+}. (b) Addition of Mg^{2+}. (c) Addition of Ni^{2+}. (d) Addition of Zn^{2+}. (e) Addition of Cu^{2+}. Peak P3 was mostly in a monomeric form for all the cases of Ca^{2+}, Mg^{2+}, Ni^{2+} and Zn^{2+}. In the cases of addition of Ca^{2+}, Mg^{2+}, and Ni^{2+} (**Figure 16a–c**, respectively), a large peak, P3, was observed at 17 min along with a small peak, P5, at 23 min. In the case of Zn^{2+} (**Figure 16d**), a large peak P3 was observed and peak P5 became very small. The chromatogram seemed to be like the case of Cu^{2+}.

of Zn^{2+}. Although there are several reports on the relationship between metal ions and the enzymatic activity of catalytic antibodies, details of the contributions of metal ions to the molecular structure of catalytic antibodies are unclear at present [20, 34]. Paul et al. reported an interesting function regarding Zn^{2+}, which was essential for exhibiting the catalytic function of the antibody light chain to cleave beta-amyloid peptides, while the ion will not affect the catalytic site [14].

4.5. Consideration about unstable forms and a stable form of CL

For the reason why the addition of copper hugely effects the formation of a mono-form structure of the constant light chain domain, we postulated one of the situations from the viewpoint of potential energy and the wall height as illustrated in **Figure 17**. It is likely that the energy

potential of each molecular form is at a comparable level after the preparation of the molecule (CL) without Cu^{2+}, as shown in **Figure 17a**. In this case, transfer of the potential well A to B (or C) is easy because the walls of the potential energies of the wells are low (**Figure 17b**). However, the energy potential is drastically changed when copper ions are added. The multi-molecular forms of the constant region domain, which are sitting in each potential well, drop in one deep potential energy level, as shown in **Figure 17c**, resulting in the formation of a mono-molecular form from the multi-molecular forms. Once the molecule dropped into the deep potential well, the form would be no longer able to transfer to other forms. As a consequence, the monomolecular form of the constant region domain molecule became stable. This situation can be achieved by the presence of copper ion in a ratio of more than 0.5 eq. of Cu^{2+} to the constant region domain molecule.
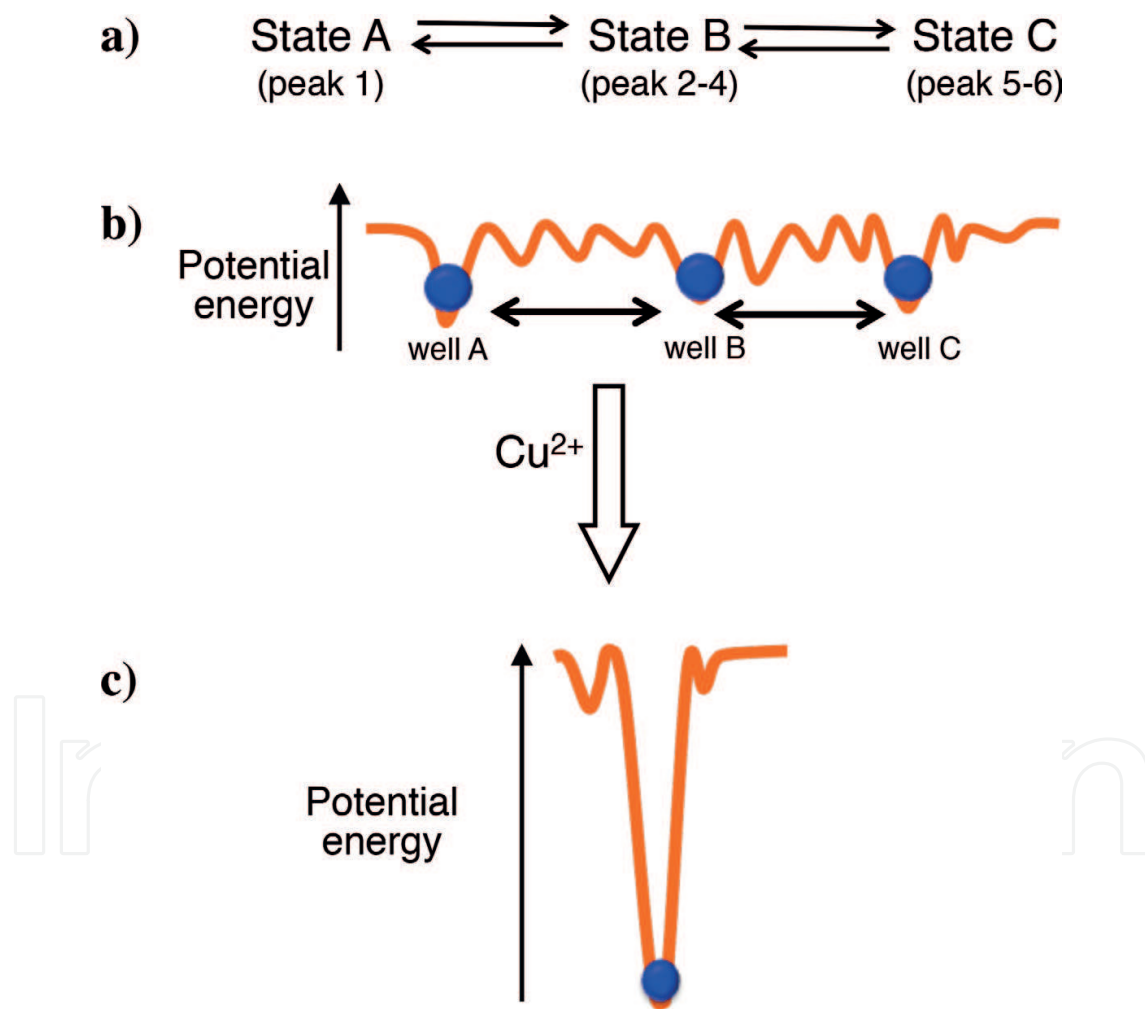

Figure 17. Consideration about conversion of unstable forms to a stable form of CL. (a) State A (corresponding to peak 1 in **Figure 10**), State B (corresponding to peaks 2, 3, and 4 in **Figure 10**), and State C (corresponding to peaks 5 and 6 in **Figure 10**) may stay in a chemical equilibrium. (b) Assumed situation in potential energy for the case without Cu^{2+}: each potential energy level for the case without Cu^{2+} may be comparable in wells of A, B, and C. The walls among the potential energy wells are not high. (c) Assumed situation of potential energy for the case with Cu^{2+}: when Cu^{2+} is incorporated, a deep potential level can be generated, and all molecules showing a different heterogeneity may drop into the well and exist as a stable form.

5. Binding of copper ions in the constant region domain

5.1. Preparation of mutants and their uptake of copper ions

In order to clarify the copper-binding site, two mutants were prepared from the C51 light chain, because the light chain has no histidine residues in the variable region compared to the sequence of the constant region domain comprising 2 His residues (**Figure 8**). Both histidine and cysteine residues are considered as the most plausible candidates for the binding site. Therefore, the residues of His195, His204, and Cys220 present in the constant region domain of the C51 light chain were mutated to Ala. As the consequence, two mutants were made. One is Cys220Ala (C220A: mono-mutant) and another is His195Ala, His204Ala, and Cys220Ala (H195A/H204A/C220A: triple-mutant; **Figure 18a**). The locations of the mutated residues are shown in **Figure 18b**.
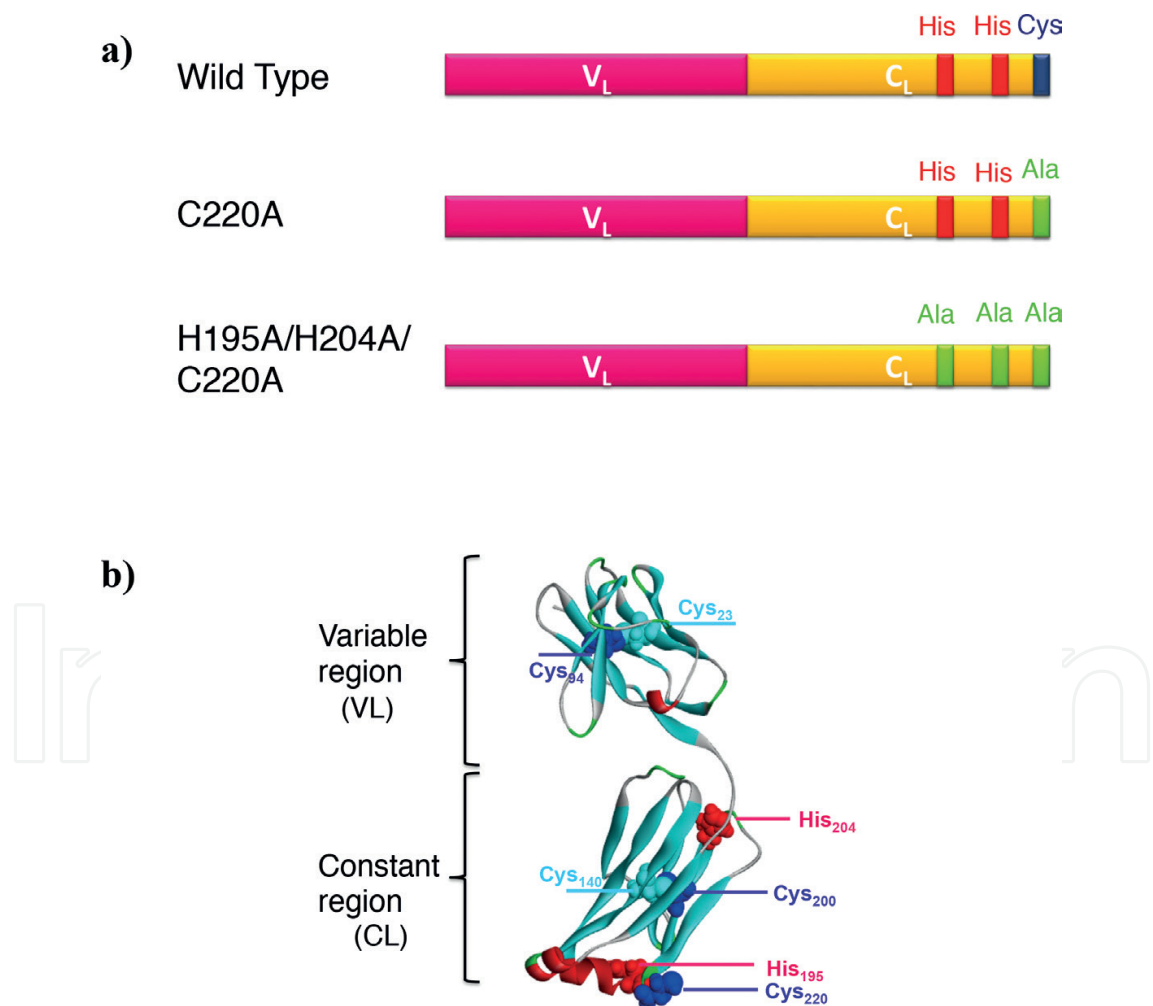

Figure 18. C51 mutants and locations of His and Cys residues. There are no histidine residues in the variable region of the C51 light chain. (a) Location of Cys220, His195 and His204 in wild type. The mutated positions, C220A and H195A/H204A/C220A, are also indicated with green colored character. (b) Three-dimensional structure of the C51 light chain. Light blue is sheet structure and red is helix structure.

These mutants were similarly expressed and purified as stated in the previous experiments. Fifty μM of Cu^{2+} (1.25 eq.) was added to both the cell suspension and the Ni-NTA eluent, where all light chains gave a single peak in the cation exchange chromatography. The copper uptake by the wild type and each mutant was chemically analyzed and the results are presented in **Table 2**. The wild type possessed 0.75 atoms of Cu^{2+} per one C51 light chain of full length. That of the C220A and H195A/H204A/C220A mutant was 0.54 and 0.25, respectively.

As stated in the above section, the value in the case of the constant region domain was 0.55. Taking together this finding and the full-length cases into account, it is considered that the variable region domain uptakes 0.20 atom (0.75–0.55 = 0.20). Therefore, the mono-mutant C220A is supposed to bind with 0.34 atom-Cu (0.54–0.20 = 0.34) and the triple-mutant H195A/H204A/C220A 0.05 atom-Cu (0.25–0.20 = 0.05). These facts are strongly implying that histidine residues at positions 195th and 204th as well as cysteine at position 220th are responsible for the copper-binding site.

5.2. Possibility of a zinc finger in the constant region domain

It is not well known that there is a zinc finger-like motif in the constant region of the antibody light chain. Interestingly, Radulescu pointed out that the motif is a type of Cys-X_3-His [35]. The sequence Cys-X_3-His-X_{15}-Cys-X_3-His is a complete motif of a zinc finger. The aa sequence of the constant region domain used in this article is presented in **Figure 8**. The sequence from positions 190th–224th of the constant region domain is CEVTHQGLSSPVTKSFNRGECLEHH. The sequence of LEHH was adducted as a His-tag was introduced. The underlined amino acids agree with those of the zinc finger motif, Cys-X_3-His-X_{15}-Cys-X_3-His, in which His224 is a part of the His-tag. This motif can uptake a metal ion such as Zn^{2+}, which is a divalent metal ion. As Cu^{2+} is also a divalent metal ion, it can bound to the motif. Based on the results of the chemical analysis of copper ions in mutants, those histidine and cysteine residues must be responsible to uptake the copper ion. It is plausible that a copper ion is able to bind to the zinc finger motif instead of a zinc ion. As seen in the investigation of divalent metal ions on the structural diversity, zinc ions showed some effect. This maybe ascribed to the presence

Clone name of C51	Cu / full length	Cu / CL	Contribution* By VL
Wild Type	0.75*	0.55*	0.20**
C220A	0.54*	0.34**	0.20***
H195A/H204A/C220A	0.25*	0.05**	0.20***

*Result: The ratio of full length of C51 vs Cu and the constant region domain of the light chain (CL) vs Cu was 0.75 and 0.55, respectively. This result suggests that the contribution of the variable domain of the light chain (VL) should be 0.20 atom. (0.75-0.55)=0.20)
  **: calculation
 ***: assumption

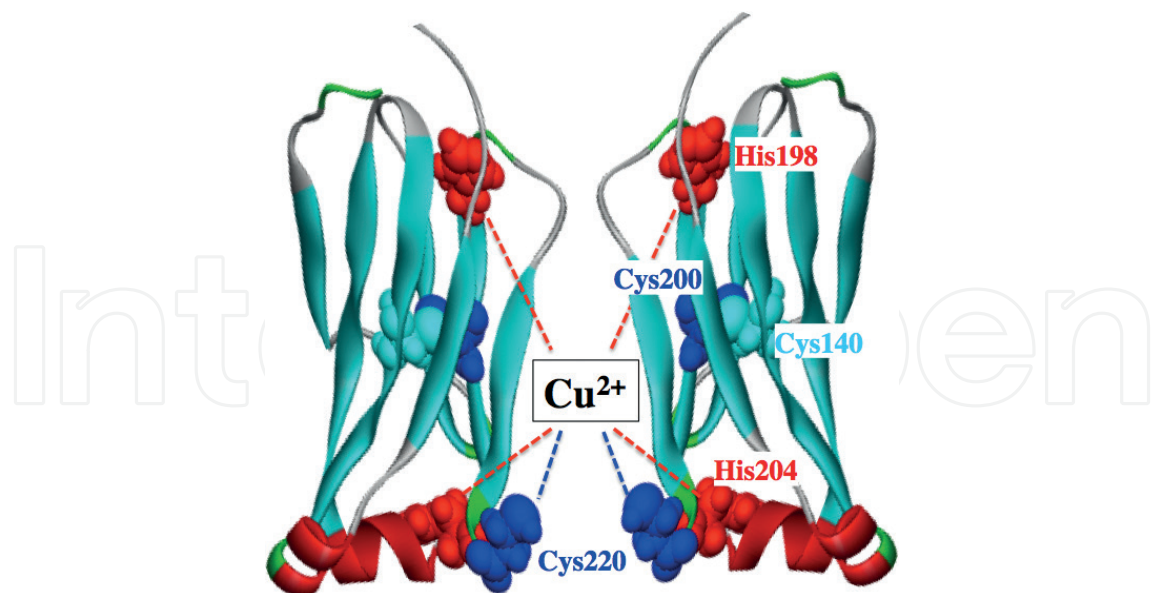**Table 2.** Copper uptake by each light chain and constant region domain (CL).

Figure 19. Assumed binding site for copper ion. A zinc finger motif, Cys-X_3-His-X_{15}-Cys-X_3-His, from positions 190th to 224th (His224 is a part of a His-tag) is existing in the constant region domain of the light chain (CL). As Cu^{2+} is also a divalent metal ion, it can be bound with the motif instead of a zinc ion, unless the ion is present in the solution. By the addition of copper ions, the CL is easily becoming the dimer form. Considering the chemical analysis of copper ions, one copper atom binds with two CL molecules (CL1 and CL2) via His and Cys residues.

of a zinc finger motif in the constant domain in the light chain (note that the zinc finger motif is conserved in both human and mouse antibody light chain (kappa type)). In addition, the similar motif composed of the same amino acids exists in the CH1 domain of the heavy chain.

As well known, a zinc finger can function as a transcription factor influencing gene regulation and protein expression. Few studies on the relationship between antibody and zinc finger have been made so far. From the viewpoint that one protein can have dual or multi-functions in case, the chemical and biochemical functions of each domain of an antibody should be investigated in detail.

5.3. Assumed binding site of a copper ion

Taking those facts mentioned above and discussed, the binding site of copper is assumed as illustrated in **Figure 19**. Cu^{2+} must be coordinated with histidine and cysteine residues of dimeric CL molecules. In this situation, the copper ion mediates the CL molecule placing the lowest potential energy level.

6. Molecular forms

6.1. AFM analysis

AFM analysis was performed using the #4 light chain as shown in **Figure 20a–g**. **Figure 20a, c,** and **e** demonstrates the wild type of the #4 light chain. The results obtained with the mutant (C220A) of the #4 light chain are shown in **Figure 20f** and **g**. The red circles in the figures represent the clear image of the AFM.

In the case of the #4 wild type, two kinds of form were observed. One is the dimer circled with #1 red color (**Figure 20a**). This seems to be a *cis* form, whose molecular conformation corresponds to that of **Figure 20b**. A variable region faces to another variable region. On the other hand, the dimer circled with #2 red color (**Figure 20c**) seems *trans* form, whose molecular conformation corresponds to that of **Figure 20d**. **Figure 20e** was another spot, where *cis* and *trans* forms were observed. In contrast, a very simple form was observed in the case of #4 mutant C220A, as shown in **Figure 20f** and **g**. In any spots, only monomeric forms were observed.

If copper ion is incorporated into the zinc finger motif residing in the constant region domain, the dimeric form observed in the #4 wild type is easily formed. On the other hand, the mutant C220A exists as the monomeric form, which indicates that the cysteine locating at position 220th is a crucial amino acid to bind to a copper ion.
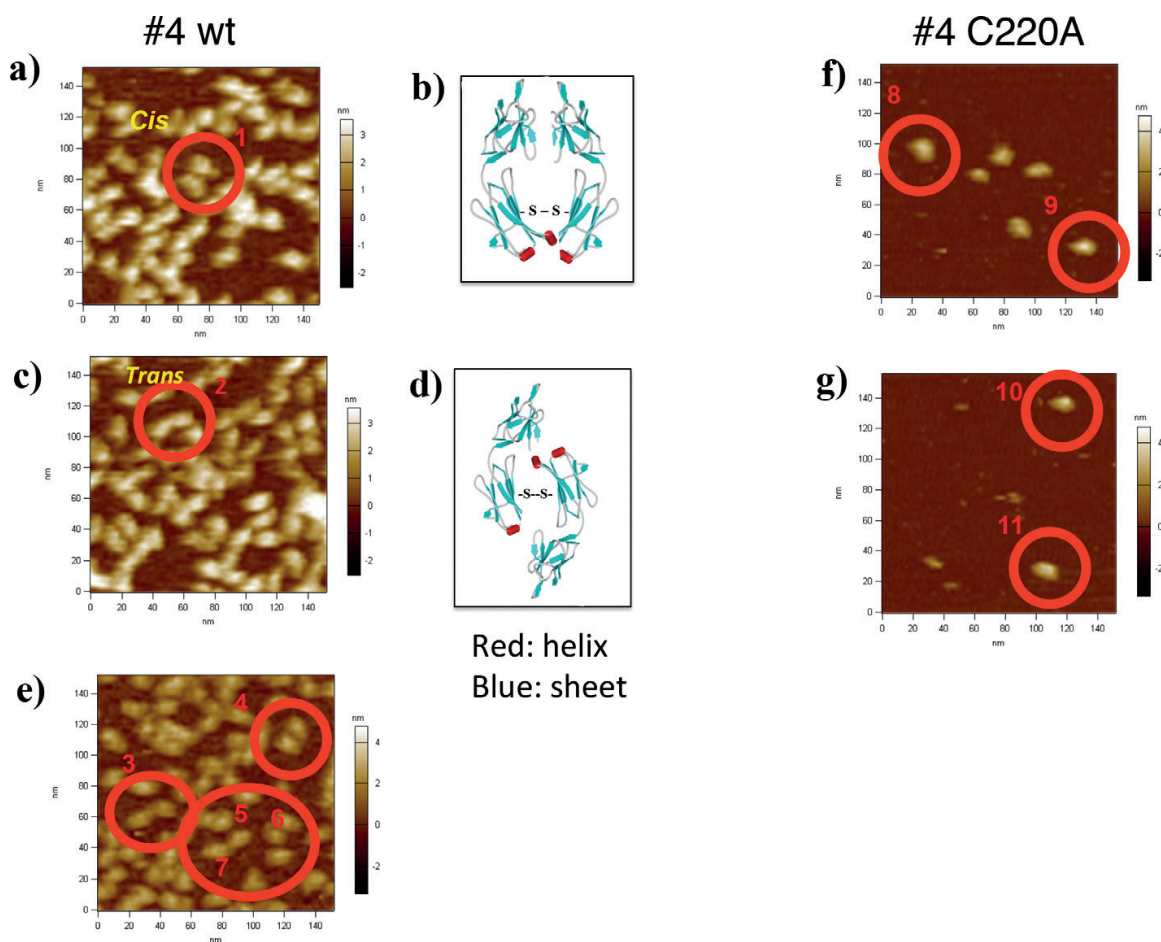

Figure 20. AFM analysis for #4 light chains. These AFM images were taken under the same condition as in **Figure 7**. (a) #4 wild type (*cis form*). (b) Molecular modeling for *cis form*. (c) #4 wild type (*trans form*). (d) Molecular modeling for *trans form*. (e) Mixture of *cis and trans forms*. In the case of the #4 wild type, two kinds of forms were observed. One is the dimer circled with #1 red color (a). This seems to be a *cis* form, whose molecular conformation corresponds to that of (b). A variable region faces to another variable region. The dimer circled with #2 red color (c) seems to be a *trans* form, whose molecular conformation corresponds to that of (d). **Figure 20e** was another view, where *cis* and *trans* forms were observed. (f) #4 mutant (C220A). (g) #4 mutant (C220A) (another spot). For #4 mutant (C220A), one simple form was observed. In any views, only monomeric forms were observed.

6.2. X-ray diffraction analysis

We are trying to determine the detailed steric conformation of a catalytic light chain. At present, the structure of the main chain of the #4 mutant C220A was clarified as a preliminary experiment. **Figure 21a** shows a single crystal of the #4 mutant C220A formed in the experiment. By using the single crystal, X-ray diffraction analysis was performed. The result is presented in **Figure 21b**, where a 3.1 Å resolution was attained. Interestingly, there are eight molecules of the #4 mutant in one lattice mediated by hydrophobic interaction.
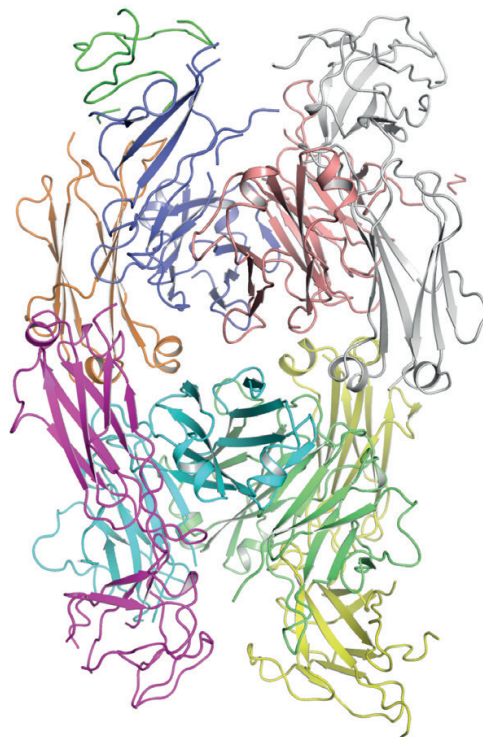
a)
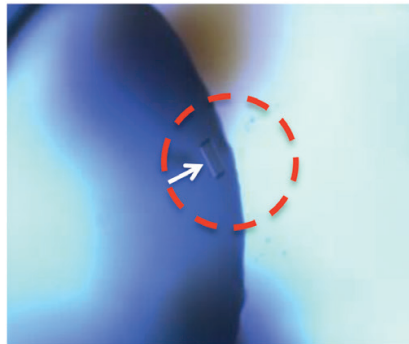
b)

Figure 21. X-ray diffraction analysis for #4 C220A. (a) crystallization: a single crystal (like a small pillar) of the #4 mutant C220A is seen in a red dotted circle. (b) Conformation of the main chain: As the preliminary experiment, the conformation of the main chain for the #4 mutant 220A was determined. Each #4 mutant molecule is indicated with each color such as red, yellow, green, blue, etc. Eight molecules of the mutant were packed in one lattice, indicating that the mutant molecules may interact with each other by hydrophobic interaction.

In the case of the AFM analysis, the #4 mutant C220A was a monomer. This is ascribed that the mica as the supporting material firmly interacts with the #4 mutant molecule. In solution, the #4 mutant may interact with each other with a strong Van der Waals force.

7. Perspectives and conclusions

As stated in the abstract and introduction, the issue of structural diversity (heterogeneity) of antibodies has become a big subject along with the development of antibody drugs and catalytic antibodies. This subject has not been solved for a long period, because many difficult and complex problems were existing. For this long-period unsolved problem, copper ion showed a drastic effect and gave one of the answers for solving the structural diversity issue. Note that the antibody and/or the subunits must have a defined structure for practical use.

In recent years, many possibilities of the development of antibody drugs and catalytic antibodies have been reported by research groups throughout the world. This article offers huge insights into the development of catalytic antibodies, maybe, as well as antibody drugs. Because the preparation can be standardized, many scientists and engineers will easily be able to produce the defined structure and the same functional antibody under any circumstances and anywhere in the world.

Acknowledgements

Author details

Emi Hifumi[1], Hiroaki Taguchi[2], Ryuichi Kato[3], Mitsue Arakawa[4], Yoshiki Katayama[5] and Taizo Uda[6,7]*

*Address all correspondence to: uda@oita-u.ac.jp

1 Research Promotion Institute, Oita University, Oita-shi, Oita, Japan

2 Faculty of Pharmaceutical Sciences, Suzuka University of Medical Science, Suzuka, Mie, Japan

3 High Energy Accelerator Research Organization, Tsukuba, Japan

4 Tottori College of Nursing, Kurayoshi-shi, Tottori, Japan

5 Graduate School of System Life Science, Kyushu University, Nishi-ku, Fukuoka, Japan

6 Department of Applied Chemistry, Faculty of Engineering, Oita University, Oita-shi, Oita, Japan

7 Nanotechnology Laboratory, Institute of Systems, Information Technologies and Nanotechnologies (ISIT), Fukuoka, Japan

References

[1] Hortobagyi NG. Trastuzumab in the treatment of breast cancer. The New England Journal of Medicine. 2005;**353**:1734-1736

[2] Glassy CM, Hagiwara H. Summary analysis of the pre-clinical and clinical results of brain tumor patients treated with pritumumab. Human Antibodies. 2009;**18**:127-137

[3] Meza-Junco J, Au H-J, Sawyer BS. Critical appraisal of trastuzumab in treatment of advanced stomach cancer. Cancer Management and Research. 2011;**3**:57-64

[4] Matsuura K, Ikoma S, Yoshida K, Shinohara H. DNA hydrolyzing activity of Bence Jones proteins. Biochemical and Biophysical Research Communications. 1998;**243**:719-721

[5] Lacroix-Desmazes S, Sooryanarayana MA, Bonnemain C, Stieltjes N, Pashov A, Sultan Y, Hoebeke J, Kazatchkine MD, Kaveri SV. Catalytic activity of antibodies against factor VIII in patients with hemophilia A. Nature Medicine. 1999;**5**:1044-1047

[6] Hifumi E, Mitsuda Y, Ohara K, Uda T. Targeted destruction of the HIV-1 coat protein gp41 by a catalytic antibody light chain. Journal of Immunological Methods. 2002;**269**:283-298

[7] Paul S, Karle S, Planque S, Taguchi H, Nishiyama Y, Handy B, Salas M, Edmundson A, Hanson A. Naturally occurring proteolytic antibodies selective immunoglobulin M-catalyzed hydrolysis of HIV gp120. The Journal of Biological Chemistry. 2004;**279**: 39611-39619

[8] Planque S, Nishiyama Y, Taguchi H, Salas M, Hanson C, Paul S. Catalytic antibodies to HIV: Physiological role and potential clinical utility. Autoimmunity Reviews. 2008;**7**:473-479

[9] Wootla B, Mahendra A, Dimitrov J-D, Friboulet A, Borel-Derlon A, Rao D-N, Uda T, Borg J-Y, Bayry J, Kaveri S-V, Lacroix-Desmazes S. Factor VIII-hydrolyzing IgG in acquired and congenital hemophilia. FEBS Letters. 2009;**583**:2565-2572

[10] Durova OM, Vorobiev II, Smirnov IV, Reshetnyak AV, Telegin GB, Shamborant OG, Orlova NA, Genkin DD, Bacon A, Ponomarenko NA, Friboulet A, Gabibov AG. Strategies for induction of catalytic antibodies toward HIV-1 glycoprotein gp120 in autoimmune prone mice. Molecular Immunology. 2009;**47**:87-95

[11] Parkhomenko TA, Buneva VN, Tyshkevich OB, Generalov II, Doronin BM, Nevinsky GA. DNA-hydrolyzing activity of IgG antibodies from the sera of patients with tick-borne encephalitis. Biochimie. 2010;**92**:545-554

[12] Hifumi E, Higashi K, Uda T. Catalytic digestion of human tumor necrosis factor-α by antibody heavy chain. The FEBS Journal. 2010;**277**:3823-3832

[13] Smirnov I, Carletti E, Kurkova I, Nachon F, Nicolet Y, Mitkevich VA, Débat H, Avalle B, Belogurov AA Jr, Kuznetsov N, Reshetnyak A, Masson P, Tonevitsky AG, Ponomarenko N, Makarov AA, Friboulet A, Tramontano A, Gabibov A. Reactibodies generated by kinetic selection couple chemical reactivity with favorable protein dynamics. Proceedings of the National Academy of Sciences of the United States of America. 2011;**108**:15954-15959

[14] Nishiyama Y, Taguchi H, Hara M, Planque SA, Mitsuda Y, Paul S. Metal-dependent amyloid β-degrading catalytic antibody construct. Journal of biotechnology. 2014;**180**:17-22

[15] Hifumi E, Honjo E, Fujimoto N, Arakawa M, Nishizono A, Uda T. Highly efficient method of preparing human catalytic antibody light chains and their biological characteristics. The FASEB Journal. 2012;**26**:1607-1615

[16] Hifumi E, Fujimoto N, Arakawa M, Saito E, Matsumoto S, Kobayashi N, Uda T. Biochemical features of a catalytic antibody light chain, 22F6, prepared from human lymphocytes. The Journal of Biological Chemistry. 2013;**288**:19558-19568

[17] Hifumi E, Morihara F, Hatiuchi K, Okuda T, Nishizono A, Uda T. Catalytic features and eradication ability of antibody light-chain UA15-L against *Helicobacter pylori*. The Journal of Biological Chemistry. 2008;**283**:899-907

[18] Kou J, Yang J, Lim J-E, Pattanayak A, Song M, Planque S, Paul S, Fukuchi K-I. Catalytic immunoglobulin gene delivery in a mouse model of Alzheimer's disease: Prophylactic and therapeutic applications. Molecular Neurobiology. 2014;**51**:43-56

[19] Hifumi E, Arakawa M, Matsumoto S, Yamamoto T, Katayama Y, Uda T. Biochemical features and anti-viral activity of a monomeric catalytic antibody light chain 23D4 against influenza A virus. The FASEB Journal. 2015;**29**:2347-2358

[20] Odintsova E-S, Zaksas N-P, Buneva V-N, Nevinsky G-A. Metal dependent hydrolysis of β-casein by sIgA antibodies from human milk. Journal of Molecular Recognition. 2010;**24**:45-59

[21] Buneva VN, Kanyshkova TG, Vlassov AV, Semenov DV, Khlimankov D, Breusova LR, Nevinsky GA. Catalytic DNA- and RNA-hydrolyzing antibodies from milk of healthy human mothers. Applied Biochemistry and Biotechnology. 1998;**75**:63-76

[22] Saveliev AN, Ivanen DR, Kulminskaya AA, Ershova NA, Kanyshkova TG, Buneva VN, Mogelnitskii AS, Doronin BM, Favorova OO, Nevinsky GA, Neustroev KN. Amylolytic activity of IgM and IgG antibodies from patients with multiple sclerosis. Immunology Letters. 2003;**86**(3):291-297

[23] Ramsland RA, Terzyan SS, Cloud G, Bourne CR, Farrugia W, Tribbick G, Geysen HM, Moomaw CR, Slaughter CA, Edundson AB. Crystal structure of a glycosylated Fab from

an IgM cryoglobulin with properties of a natural proteolytic antibody. The Biochemical Journal. 2006;**396**:473-481

[24] Harris RJ, Kabakoff B, Macchi FD, Shen FJ, Kwong M, Andya JD, Shire SJ, Bjork N. Identification of multiple sources of charge heterogeneity in a recombinant antibody. Journal of Chromatography B. 2001;**752**:233-245

[25] Nebija D, Noe CR, Urban E, Lachmann B. Quality control and stability studies with the monoclonal antibody, trastuzumab: Application of 1D- *vs.* 2D-gel electrophoresis. International Journal of Molecular Sciences. 2014;**15**:6399-6411

[26] Stevens FJ, Westholm FA, Solomon A, Schiffer M. Dual conformations of an immuno-globulin light-chain dimer: Heterogeneity of antigen specificity and idiotope profile may result from multiple variable-domain interaction mechanisms. Proceedings of the National Academy of Sciences of the United States of America. 1988;**85**:6895-6899

[27] Hunt G, Moorhouse KG, Chen AB. Capillary isoelectric focusing and sodium dodecyl sulfate capillary gel electrophoresis of recombinant humanized monoclonal; antibody HER2. Journal of Chromatography. A. 1996;**744**:295-301

[28] Fujimoto N, Hifumi E, Uda T. Biochemical features of monoclonal antibodies (InfA series) against hemagglutinin molecule of influenza virus. Proceedings (J1-52) of Annual Meeting of the Chemical Society of Japan. 2009

[29] Hifumi E, Fujimoto N, Ishida K, Kawawaki H, andT. Uda, T. Characteristic features of InfA-15 monoclonal antibody recognizing H1, H3 and H5 subtypes of hemagglutinin of influenza virus A type. Journal of Bioscience and Bioengineering. 2010;**109**:598-608

[30] Nebija D, Kopelent-Frank H, Urban E, Noe CR, Lachmann B. Comparison of two-dimen-sional gel electrophoresis patterns and MALDI-TOF MS analysis of therapeutic recombi-nant monoclonal antibodies trastuzumab and rituximab. Journal of Pharmaceutical and Biomedical Analysis. 2011;**56**:684-691

[31] Hifumi E, Matsumoto S, Nakashima H, Itonaga S, Arakawa M, Katayama Y, Kato R, Uda T. A novel method of preparing the mono-form structure of catalytic antibody light chain. FASEB Journal. 2016;**30**:895-908

[32] Hifumi E, Taguchi H, Kato R, Uda T. Role of the constant region domain in the structural diversity of human antibody light chains. FASEB Journal. 2017;**31**:1668-1677

[33] Ouerghi O, Touhami A, Othmane A, Ouada HB, Martelet C, Fretigny C, Jaffrezic-Renault N. Investigating antibody–antigen binding with atomic force microscopy. Sensors and Actuators B: Chemical. 2002;**84**(2-3):67-175

[34] Bezuglova AM, Konenkova LP, Doronin BM, Buneva VN, Nevinsky GA. Affinity and catalytic heterogeneity and metal-dependence of polyclonal myelin basic protein-hydrolyzing IgGs from sera of patients with systemic lupus erythematosus. Journal of Molecular Recognition. 2011;**24**:960-974

[35] Radulescu RT. Antibody constant region: Potential to bind metal and nucleic acid. Medical Hypotheses. 1995;**44**:137-145